Electron cyclotron plasma breakdown in tokamaks: validation on KSTAR and implications for ITER-like devices

Jinwoo Gwak[1], Min-Gu Yoo[2], Jeongwon Lee[3], Yeongsun Lee[1,4], Hyun-Tae Kim[5], and Yong-Su Na[1*]

[1] *Department of Nuclear Engineering, Seoul National University, Seoul, Republic of Korea*

[2] *General Atomics, San Diego, CA 92186-5608, USA*

[3] *Korea Institute of Fusion Energy, Daejeon, Republic of Korea*

[4] *Nuclear Research Institute for Future Technology and Policy, Seoul, Republic of Korea*

[5] *United Kingdom Atomic Energy Authority, Culham Campus, Abingdon, Oxfordshire OX14 3DB, United Kingdom*

[*]Corresponding author: ysna@snu.ac.kr

Introduction In reactor-scale tokamaks, the low electrical resistance of the vacuum vessel makes purely inductive breakdown onset difficult to predict [1], motivating interest in non-inductive breakdown. Injection of electron cyclotron (EC) waves is a widely investigated non-inductive start-up approach in present-day devices [2]. Experiments have demonstrated that EC waves can initiate plasma breakdown (pre-ionization) even prior to the application of a loop voltage [3]. Extending EC breakdown to future devices, however, requires a predictive framework capable of quantifying operational requirements such as minimum EC beam power, prefill pressure, and connection length in advance.

`BREAK` is a 3D particle-in-cell code developed for tokamak plasma breakdown simulations, treating collisional processes, ionization, and boundary losses [4]. In Ref. [5], localized EC wave–particle interaction and resultant energy-gain models [6, 7] were incorporated into `BREAK`. The EC energy exchange is thereby treated as a fast microscopic process, separated from the slower macroscopic evolution of the discharge. This enables quantitative prediction of the EC breakdown boundary, but experimental comparison of the model has not yet been established.

In this work, we compare the EC breakdown boundary observed as a function of prefill pressure and connection length on KSTAR with the corresponding simulation predictions, to assess the prediction capability of the model. The same framework is then applied to project the operating space for an ITER-like device.

Model During the early phase of microwave breakdown, a seed electron gains energy through nonlinear EC wave–particle interaction, while the absorbed EC power remains a negligible fraction of the launched power. This interaction, together with electron–neutral elastic collisions, ionization, and boundary losses, is implemented in the 3D particle-in-cell code `BREAK`, in which particle orbits advance in a prescribed magnetic geometry; the underlying assumptions and their verification are detailed in Refs. [7, 5]. A case is classified as successful breakdown when the

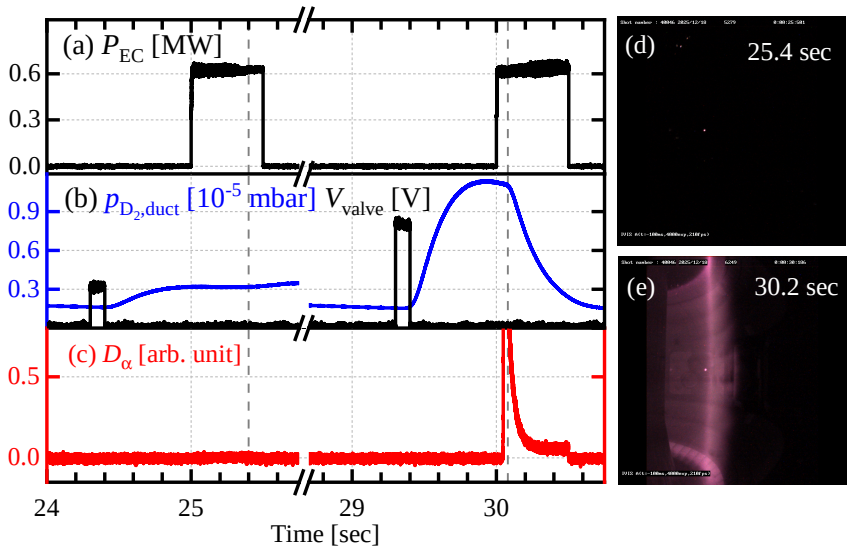

Figure 1: Representative time window from KSTAR shot #40046. (a) Injected EC power P_{EC}. (b) D_2 pressure measured in the vacuum duct in front of the gas pump (blue) and gas-puff valve voltage V_{valve} (black). (c) Raw D_α signal from a representative channel. The broken time axis shows two successive EC pulses within the same discharge. (d),(e) Visible-light camera frames at the times marked by dashed lines in (a)–(c), showing no plasma formation and successful breakdown, respectively.

electron population in $\mathscr{R}$ exhibits sustained multiplication at a rate $d\ln\langle n_e\rangle_{\mathscr{R}}/dt > 100\ \mathrm{s}^{-1}$. Here, $\mathscr{R}$ refers to the resonance-layer region where cold electrons undergo nonlinear EC wave–particle interaction [8], and $\langle\cdot\rangle_{\mathscr{R}}$ denotes the average over the toroidal volume enclosed by $\mathscr{R}$.

Experiments Figure 1 shows a representative time window of a KSTAR discharge in which successive EC pulses, each preceded by a programmed D_2 puff, were applied to test EC breakdown under zero loop voltage. The toroidal magnetic field was fixed at $B_0 = 1.8$ T at $R_0 = 1.8$ m. The externally imposed vacuum poloidal field was also held fixed during each EC pulse. EC power was supplied by a single 105-GHz gyrotron and launched in X mode from the low-field side. The launched power was 0.6 MW for 0.5 s per pulse, with a beam width of 5 cm at the resonance layer estimated from a dedicated ray-tracing calculation. The toroidal launch angle was $\approx 5^\circ$, corresponding to near-normal incidence, as constrained by in-vessel protection. The poloidal steering was chosen so that the beam intersected the X2 resonant layer near the midplane. With this fixed launch geometry, prefill-pressure scans were performed at two designed-L_c environments. Two vertical-field configurations were used to vary L_c while minimizing $E \times B$-transport effects, giving $L_c = 110$ and 58.8 m as calculated with the `FIST99` code [9]. The prefill pressure was scanned by varying the puff-command voltage [Fig. 1(b)]. Breakdown was identified when the raw D_α signal rose above the noise floor in any toroidal or poloidal channel during the pulse [Fig. 1(c)].

To demonstrate the prediction capability of the breakdown onset criteria, we performed

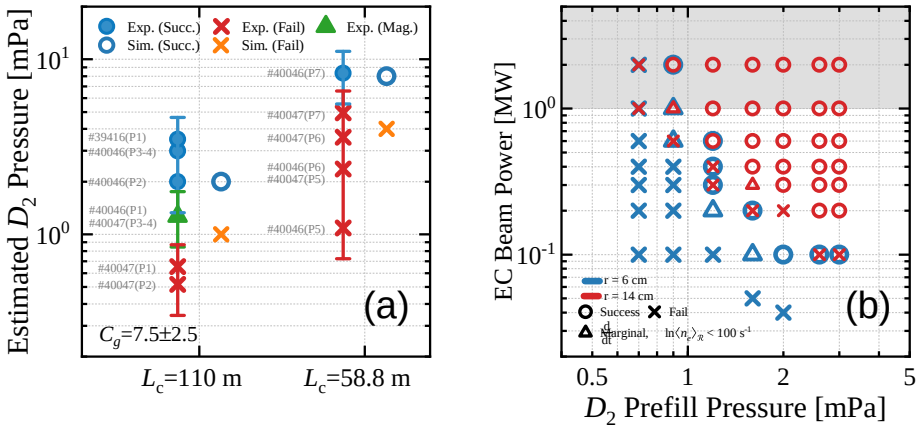

Figure 2: **(a)** EC breakdown results on KSTAR at $L_c = 110$ and 58.8 m. Blue filled circles, red crosses, and green filled triangles mark successful, failed, and delayed marginal cases in the experiment; open blue circles and orange crosses mark predicted success and failure. Vertical bars indicate the pressure uncertainty from the vessel-to-duct conversion factor C_g. Gray labels denote the shot number and EC-pulse index (e.g., #40047(P1)); markers within each L_c group are displaced horizontally for clarity. **(b)** Predicted pressure–power scan for ITER-like EC breakdown, with $B_0 = 2.65$ T at $R_0 = 6.2$ m and $\omega = 2\pi \times 170$ GHz. Blue and red symbols correspond to beam radii $r = 6$ and 14 cm at resonance. Open circles, crosses, and open triangles mark successful, failed, and marginal cases ($0 < d\ln\langle n_e\rangle_{\mathscr{R}}/dt < 100\ \mathrm{s}^{-1}$). Gray shading indicates $P_{\mathrm{EC}} > 1$ MW.

prefill-pressure scans using particle simulations. The simulations considered the KSTAR-like domain and the experimental EC parameters described above, with a uniform, static B_Z chosen to reproduce the corresponding L_c for each vertical-field configuration. The wave incidence was taken to be perpendicular because the experimental launch satisfies $|N_\parallel| \lesssim 0.1$ at the resonance, and the corresponding correction to the nonlinear cold-electron energy gain is below 6% and is therefore neglected.

Figure 2(a) compares the experimental classification with the numerical prediction as a function of the inferred in-vessel D_2 prefill pressure for the two L_c settings. Repeated experimental pulses at the condition marked by the green triangle produced both failures and delayed breakdowns— onset delayed by several hundred milliseconds — under nominally identical programmed settings. Because the gauge is located closer to the gas pump than to the vessel, the duct pressure underestimates the in-vessel pressure, and we relate the two by $p_0 = C_g\, p_{\mathrm{D_2,duct}}$ with a conversion factor $C_g > 1$. With $C_g = 7.5 \pm 2.5$, the predicted failures lie in the observed failure range and the predicted breakdowns lie in the observed breakdown range, within the inferred-pressure uncertainty, for both L_c environments. A Monte-Carlo simulation of molecular dynamics is being undertaken to confirm the conversion factor, but it's not shown here.

ITER-like projection Figure 2(b) shows the predicted EC-breakdown boundary for an ITER-like device, whose magnetic geometry and EC beam parameters follow ITER plasma-initiation

conditions [1, 10], with beam radii $r = 6$ and 14 cm spanning the ITER EC-launcher range [10]. In a realistic EC breakdown, a null configuration has a small stray field across the field null. Hence, an ideal estimate of the connection length L_c necessitates the full magnetic field configuration. Instead, we simply introduce the proxy vertical field $B_Z = B_{\mathrm{pol}}/f_{\mathrm{null}} \simeq 170$ G, for which the effective connection length $\widetilde{L}_c = f_{\mathrm{null}}|Z|_{\max}B_{\mathrm{res}}/B_{\mathrm{pol}}$ represents the characteristic loss scale of the ITER field-null start-up. Here $|Z|_{\max} = 1.6$ m is the vertical half-extent of the simulation domain. The value $B_{\mathrm{pol}} = 30$ G denotes the level of the residual poloidal magnetic field that ITER aims to achieve in the breakdown region [1], and f_{null} is the geometric reduction factor required for compensating the proxy treatment. This factor barely varies across field-null configured tokamaks, so we choose $f_{\mathrm{null}} = 0.18$ obtained from the calibration against the DIII-D EC-breakdown threshold of Ref. [11].

Successful avalanches are obtained near and below $P_{\mathrm{EC}} = 1$ MW at $p_{\mathrm{D_2}} \simeq 2$ mPa, indicating that ITER-like EC breakdown remains accessible at modest beam power. Because this projection is obtained from an integrated simulation that combines wave–particle interaction, transport, and loss, work is ongoing to isolate the individual physical mechanisms and thereby clarify the underlying physics that sets this boundary.

Summary The EC breakdown boundary observed on KSTAR as a function of prefill pressure and connection length is found to be consistent with particle-simulation predictions, providing the first experimental comparison of this model. The same framework projects successful EC breakdown near and below 1 MW at $p_{\mathrm{D_2}} \simeq 2$ mPa for an ITER-like device, within the output of a single ITER EC gyrotron.

References

[1] P.C. de Vries and Y. Gribov, Nucl. Fusion **59**, 096043 (2019).

[2] J. Stober *et al.*, Nucl. Fusion **51**, 083031 (2011).

[3] G.L. Jackson, J.S. deGrassie, C.P. Moeller and R. Prater, Nucl. Fusion **47**, 257 (2007).

[4] M.-G. Yoo, J. Lee, Y.-G. Kim *et al.*, Nat. Commun. **9**, 3523 (2018).

[5] J. Gwak *et al.*, in *Proc. 30th IAEA Fusion Energy Conf.* (2025), IAEA-CN-316/2994.

[6] D. Farina, Nucl. Fusion **58**, 066012 (2018).

[7] J. Gwak, *et al.*, Nucl. Fusion **65**, 056038 (2025).

[8] D. Farina, EPJ Web Conf. **203**, 01001 (2019).

[9] J. Kim, S.W. Yoon, Y.M. Jeon *et al.*, Nucl. Fusion **51**, 083034 (2011).

[10] A. Moro, A. Bruschi, O. Darcourt *et al.*, Fusion Eng. Des. **154**, 111547 (2020).

[11] J. Sinha, P.C. de Vries, M.L. Walker *et al.*, Nucl. Fusion **62**, 066013 (2022).